Optimization of a combined power plant CO_2 capture and direct air capture concept for flexible power plant operation

Electronic supplementary information (ESI)

Edward J. Graham[1], Moataz Sheha[1], Dharik S. Mallapragada[1], Howard J. Herzog[1], Emre Gençer[1], Phillip Cross[2], James Custer[2], Adam Goff[2], and Ian Cormier[2]

[1]MIT Energy Initiative, Massachusetts Institute of Technology, Cambridge, MA, USA.
[2]8 Rivers Capital, Durham, USA

Electronic supplementary information for the paper 'Optimization of a flexible carbon capture process coupled with direct air capture'. Section S1 describes the process model equations and fixed parameters used in the optimizations. Section S2 describes the equations used in the net present value calculation. Section S4 describes the method used to develop an analytical equation for the CaO conversion in the carbonator. Section S5 describes the k-means clustering algorithm that is used to reduce the time-dimensionality of the optimization model. Section S6 describes the methodology for developing a surrogate model for the membrane unit. Two other case studies are presented to support the discussion in the main text, a case where the carbon price is raised to \$200/tonne (Section S7), and another case where all gases are recycled from the separation units to the carbonator (Section S8). Finally, in Section S9 we provide further information for the MiNg \$150 PJM scenario.

S1 Process Model

A schematic of the process model is shown in the main text (Figure 1). Variables used in this section are defined in Table S1. Model parameters are defined in Tables S2 and S4.

Table S1 List of variables used within the optimization model.

Variable	Description	Units
Process variables		
$F_t^{NG,PP}$	Natural gas flowrate to NGCC plant	MMol $^{-1}$
$F_{i,j,t}^{s}$	Molar flowrate of stream i and component j at time t	MMol hr^{-1}
$F_{i,t}^{s,tot}$	Total molar flowrate of stream i	MMol hr^{-1}
$z_{i,j,t}^{s}$	Mole fraction of stream i and component j at time t	-
$F_{i,j,t}^{gl}$	Molar flowrate of stream i and component j at time t	MMol hr^{-1}
$F_{i,t}^{gl,tot}$	Total molar flowrate of stream i	MMol hr^{-1}
$z_{i,j,t}^{gl}$	Mole fraction of stream i and component j at time t	-
$F_{i,j,t}^{b}$	Molar flowrate of stream i and component j at time t	MMol hr^{-1}
$F_{i,t}^{b,tot}$	Total molar flowrate of stream i	MMol hr^{-1}
$z_{i,j,t}^{b}$	Mole fraction of stream i and component j at time t	-
$y_{f,CO_2,t}$	Mole fraction of CO_2 in membrane feed	
$y_{p,CO_2,t}$	Mole fraction of CO_2 in membrane permeate	
$y_{r,CO_2,t}$	Mole fraction of CO_2 in membrane retentate	
W_t	Power	GW
Q_t^u	Heat input to unit u	GW
ζ_t	Extent of reaction	MMol hr^{-1}
γ_t	Fraction of stream 3 split to carbonator	-
ϕ_t	Fraction of stream 7 split to carbonator	-
α_t	Fraction of stream 22 split to carbonator	-
P_t	Pressure of stream 17 entering the membrane	bar
$\bar{X}_t^{carb}$	Average CaO conversion in the carbonator	-
$nCaODAC_t$	Storage inventory before DAC	MMol
CaO_{use}	CaO flowrate from storage to DAC	MMol hr^{-1}
y_t	Binary variable denoting on/off state of the NGCC plant (1 is on, 0 is off)	-
s_t	Binary variable to track whether the NGCC turns on between consecutive time steps	-
A	Membrane area	Mm^2

Table S1 – continued from previous page

Variable	Description	Units
$\bar{\sigma}$	Dimensionless membrane area divided by retentate pressure (see S6)	bar^{-1}
ΔH_t	Enthalpy change between carbonator off-gas (stream 10) and the vented stream after providing heat to the dryer and HRSGG	GW
Q_t^{dryer}	Heat requirement for the dryer	GW
$Cduty_t^{PP}$	Power plant coolind duty	GW
$Cduty_t^{Carbon8}$	Cooling duty for Carbon8 system	GW
W_t^{PP}	Electricity production from power plant	GW
W_t^{HRSG}	Electricity production from HRSG	GW
W_t^{VPSA}	Electricity requirement for VPSA	GW
W_t^{CPU}	Electricity requirement for CPU	GW
W_t^{DAC}	Electricity requirement for DAC	GW
$W_t^{Compressor}$	Electricity requirement for compression before membreane	GW
Capacity/ costing variables		
$capFlow_{calciner}$	Maximum flow rate of calciner solids input (stream 2)	Mmol/hr
$capFlow_{carbonator}$	Maximum flow rate of carbonator solids input (stream 5)	Mmol/hr
$capFlow_{LimestoneMill}$	Maximum flow rate of solids exiting the limestone mill (stream 1)	Mmol/hr
$capFlow_{Blower}$	Maximum flowrate of gases entering the blower (stream 16)	Mmol/hr
$capFlow_{VPSA}$	Maximum flowrate of gases exiting the VPSA (stream 11)	Mmol/hr
$capFlow_{HRSG,turbines+generators}$	Maximum power produced by the HRSG	GW
$capFlow_{HRSG,ductwork+stack}$	Maximum power produced by the HRSG	GW
$capFlow_{MembraneCompressor}$	Maximum compression work before membrane	GW
$capFlow_{BOPCoolingWater}$	Maximum cooling water duty	GW
$cap_{DACstorage}$	Maximum storage inventory in DAC storage unit	Mmol
$flowRatio_u$	Ratio of capacity flow and base case flow (bcf_u)	-
$unitCost_u$	Cost for unit u	$M
$c_{membrane}$	Cost of membrane per unit area	$/m^2
$CAPEX_{annualized}$	Annualized total capital cost of the plant	$M
$opex_t^{CPU}$	Electricity cost for CPU	$M/hr
$opex_t^{Membrane}$	Electricity cost for membrane compression	$M/hr
$opex_t^{DAC}$	Electricity cost for DAC	$M/hr
$opex_t^{PowerPlantNG}$	Cost of natural gas to NGCC plant	$M/hr
$opex_t^{CalcinerNG}$	Cost of natural gas to Calciner	$M/hr
$opex_t^{VPSA}$	Electricity cost for VPSA	$M/hr
$opex_t^{LimestonePurchase}$	Cost of limestone purchase	$M/hr
$opex_t^{LimestoneDisposal}$	Cost of limestone disposal	$M/hr
$opex_t^{VentedGasRecycle}$	Carbon cost of venting recycled gases	$M/hr
$opex_t^{VentedGasCarbonator}$	Cost of venting off-gases from carbonator	$M/hr
$opex_t^{CO_2Sequestration}$	Cost of CO_2 sequestration	$M/hr
$opex_t^{Startup}$	Cost of starting up the NGCC plant	$M/hr
$OPEX_{var,annual}$	Total variable annual OPEX	$M/yr
$OPEX_{fixed,annual}$	Total fixed annual OPEX	$M/yr
$OPEX_{annual}$	Total annual OPEX	$M/yr
$revenue_t^{PowerPlant}$	Revenues from NGCC electricity generation	$M/hr
$revenue_t^{HRSG}$	Revenues from HRSG electricity generation	$M/hr
$revenue_t^{DAC}$	Revenues from DAC CO_2 removal	$M/hr
$REVENUE_{annual}$	Total annual revenue	$M/yr
NPV	Net present value of project	$M
Subscripts		
i	Stream	
j	Component	
t	Time	hr
Superscripts		
tot	Total flow rate	
PP	Power Plant	
$carb$	Carbonation reaction	
$calc$	Calcination reaction	
$comb$	Combustion reaction	
CAP	Maximum Capacity	

Table S1 – continued from previous page

Variable	Description	Units
gl	Gas or liquid streams	
s	Solid streams	
b	Binary mixture of CO_2 and N_2	

Table S2 List of Parameters used within the optimization model.

Parameter	Description	Value	Units
N_t	Number of hours	720	hr
$X^{CaO,DAC}$	DAC conversion	0.9	-
X^{calc}	Conversion of $CaCO_3$ in the calciner	1	-
X^{carb,CO_2}	CO_2 conversion in the carbonator	0.95	-
Flow rates/ compositions			
$F^{s}_{1,CaO,t}$	Feed CaO	0	MMol/hr
$z^{gl}_{7,CO_2,t}$	Mole fraction of flue gas	0.041	-
$z^{gl}_{7,O_2,t}$	Mole fraction of flue gas	0.121	-
$z^{gl}_{7,H_2O,t}$	Mole fraction of flue gas	0.088	-
$z^{gl}_{7,N_2,t}$	Mole fraction of flue gas	0.750	-
$z^{gl}_{7,CH4,t}$	Mole fraction of flue gas	0	-
$z^{gl}_{12,CO_2,t}$	Mole fraction of VPSA outlet	0	-
$z^{gl}_{12,O_2,t}$	Mole fraction of VPSA outlet	0.95	-
$z^{gl}_{12,H_2O,t}$	Mole fraction of VPSA outlet	0	-
$z^{gl}_{12,N_2,t}$	Mole fraction of VPSA outlet	0.05	-
$z^{gl}_{12,CH4,t}$	Mole fraction of VPSA outlet	0	-
$z^{gl}_{13,CO_2,t}$	Mole fraction of natural gas to calciner	0	-
$z^{gl}_{13,O_2,t}$	Mole fraction of natural gas to calciner	0	-
$z^{gl}_{13,H_2O,t}$	Mole fraction of natural gas to calciner	0	-
$z^{gl}_{13,N_2,t}$	Mole fraction of natural gas to calciner	0	-
$z^{gl}_{13,CH4,t}$	Mole fraction of natural gas to calciner	1	-
$c^{21}_{CO_2}$	Purity constraint for CO_2 sequestration	0.95	-
Regression coefficients			
c^{b}_{19,CO_2}	Linear coefficient for inlet CO_2 flowrate to distillation	1.2851	-
$c^{tot,b}_{19,CO_2}$	Linear coefficient for total (permeate) flowrate to distillation	-0.2425	-
c^{PP}_{1}	Coefficient for relating NGCC power to Flue gas flowrate	5.845	MMol/GWh
c^{PP}_{2}	Coefficient for relating NGCC power to Flue gas flowrate	1.0543	MMol/h
$c^{PP,CAP,min}$	Minimum stable operation of NGCC plant as a fraction of full capacity	0.4	-
$c^{NG,PP}$	Coefficient relating NGCC flue gas flowrate to natural gas flowrate	25.7	-
$c^{tot,gl}_{11}$	-	11.098	-
$c^{tot,gl}_{8}$	-	0.7411	-
$c^{tot,gl}_{12}$	-	2.036	-
$c^{tot,s}_{1}$	-	8.652	-
$c^{tot,s}_{6,CaCO_3}$	-	7.403	-
$c^{tot,s}_{6,CaO}$	-	1	-
c^{quench}	Coefficient used to determine the amount of water used in quenching	0.0457	-
$c^{waterremoval}$	Fraction of water removed by flash, compressor knockout and dryer	0.012	-
c^{Qdryer}	Thermal energy coefficient for dryer	0.0245	GW/MMol
c^{lnP}_{1}	Linear coefficient for ln P_t	0.1933	-

Table S2 – continued from previous page

Parameter	Description		Units
c_2^{lnP}	Linear coefficient for ln P_t	0.5888	-
$c^{Cduty,PP}$	Coefficient defining the relationship between power plant cooling duty and flow rate of NGCC flue gas (stream 7)	0.00295	GW/(Mmol/hr)
$c^{Cduty,Carbon8}$	Coefficient defining the relationship between Carbon8 cooling duty and flow rate of calciner off-gas (stream 14)	0.0138	GW/(Mmol/hr)
c^{comp}	Coefficient for compressor power scaling	1.138	-
c^{WVPSA}	Relation between VPSA power requirement and flow rate of stream 11	0.00842	GW/(Mmol/hr)
c^{WCPU}	Relation between CPU power requirement and permeate flowrate (stream 19)	0.492	GW/(Mmol/hr)
c^{WDAC}	Relation between DAC power requirement and CaO flowrate to DAC	0.00842	GW/(Mmol/hr)
Membrane surrogate model coefficients			
c_1^{surr}		-0.0118	bar
c_2^{surr}		0.000119	bar^2
c_3^{surr}		0.311	-
c_4^{surr}		-0.00559	bar
c_5^{surr}		0.0308	bar^-1
c_6^{surr}		2.643	-
c_7^{surr}		-2.394	-
Experimental coefficients			
$Perm_{CO_2}$	CO_2 permeance in the membrane	0.000484	MMol/hr/m^2/bar
$Perm_{N_2}$	N_2 permeance in the membrane	0.00002	MMol/hr/m^2/bar
f_m	How fast the CaO carrying capacity approaches f_w	0.7 [1]	-
f_w	Carrying capacity of CaO when the number of cycles approaches infinity	0.25 [1]	-
h_{9,H_2O}	Pure component enthalpy of flue gas stream to carbonator	-239.94	GJ/MMol
h_{9,CO_2}	Pure component enthalpy of flue gas stream to carbonator	-391.3	GJ/MMol
h_{9,O_2}	Pure component enthalpy of flue gas stream to carbonator	1.71	GJ/MMol
h_{9,N_2}	Pure component enthalpy of flue gas stream to carbonator	1.69	GJ/MMol
h_{23,CO_2}	Pure component enthalpy of gas recycle stream	-394.1	GJ/MMol
h_{23,N_2}	Pure component enthalpy of gas recycle stream	0.396	GJ/MMol
$h_{5,CaCO_3}$	Pure component enthalpy of carbonator inlet solids	-1147.8	GJ/MMol
$h_{5,CaO}$	Pure component enthalpy of carbonator inlet solids	-605.7	GJ/MMol
$h_{6,CaCO_3}$	Pure component enthalpy of carbonator outlet solids	1170.3	GJ/MMol
$h_{6,CaO}$	Pure component enthalpy of carbonator outlet solids	616.2	GJ/MMol
h_{10,H_2O}	Pure component enthalpy of vented gas after HRSG	-233.76	GJ/MMol
h_{10,CO_2}	Pure component enthalpy of vented gas after HRSG	-383.67	GJ/MMol
h_{10,O_2}	Pure component enthalpy of vented gas after HRSG	7.11	GJ/MMol
h_{10,N_2}	Pure component enthalpy of vented gas after HRSG	6.89	GJ/MMol
$c^{\eta^{HRSG}}$	Relation between HRSG power and cooling duty	0.384	-

Table S2 – continued from previous page

Parameter	Description		Units
$\bar{C}_p$	Average heat capacity of calciner off-gas before and after HRSG	0.0378	GJ/MMol/K
R	Ideal Gas Constant	0.008314	GJ/MMol.K
Design specifications			
$Q^{carb,loss}$	Fixed carbonator heat loss	10	MW
$c^{T_{15}}$	Temperature of stream 15	620	C
$c^{T_{16}}$	Temperature of stream 16 after HRSG	180	C
c^{P_0}	Compression inlet pressure	1	bar
$capFlow^{max}_{Calciner}$	Maximum flowrate of solids entering calciner (stream 2)		Mmol/hr
$c^{excess_{O_2}}$	Fraction of excess O_2 required for methane combustion	0.03	-
$z^{max,calciner}_{O_2}$	Maximum mole fraction of O_2 to calciner in gas phase	0.3	-
$W^{PP,CAP}$	NGCC power production capacity	0.74	GW
Costing parameters			
$c^{LimestonePurchase}$	Cost of feed limestone, based on \$5/tonne	0.0005	\$M/Mmol
$c^{LimestoneDisposal}$	Cost of limestone disposal, based on \$3/tonne	0.0003	\$M/Mmol
$c^{Sequestration}$	Cost of CO_2 sequestration, based on \$10/tonne	0.00044	\$M/Mmol
EP_t	Electricity price	varies based on market scenario	\$M/GW
$FuelPrice$	Fuel Price, based on 0.0224 MMBtu/lb HHV	varies based on market scenario	\$M/Mmol
$CarbonPrice$	Carbon Price	varies based on market scenario	\$M/Mmol
$c^{StartUp}$	Start up cost, based on 44\$/MW-cap (warm start)	$0.055W^{PP,CAP}$	\$M/GW^2
$c^{FixedOPEX}_1$	Fixed OPEX parameter	51.4	\$M/yr
$c^{FixedOPEX}_2$	Fixed OPEX parameter	0.02	\$M/yr/(\$M-CAPEX)
CRF	Capital Recovery Factor, based on 30 years lifetime, 7.25% discount rate	0.083	-
bcf_u	Flow rate used in the base case in the work of[3]	see table S4	(varies)
bf_u	Flow rate of unit with known cost	see table S4	(varies)
c_u	Cost of unit with known price	see table S4	\$M
e_u	Cost exponent	see table S4	-
Subscripts			
i	Stream		-
j	Component		-
t	Time		hr
u	Single or aggregated process unit		-
Superscripts			
PP	Power Plant		
CAP	Maximum Capacity		

S1.1 Power plant model

Based on detailed Aspen Plus simulations of the NGCC plant[3], we found that it was reasonable to model the net power production as a linear function of the feed natural gas flow rate. The variation in flue gas composition with respect to net power is negligible for the purpose of this work. The power plant model is given by the following set of equations:

$$F^{NG,PP}_t = (c^{PP}_1 W^{PP}_t + c^{PP}_2) y_t \tag{S1}$$

$$W^{PP}_t \geq c^{PP,CAP,min} W^{PP,CAP} y_t \tag{S2}$$

$$W^{PP}_t \leq W^{PP,CAP} y_t \tag{S3}$$

$$F^{tot,gl}_{7,t} = c^{NG,PP} F^{NG,PP}_t \tag{S4}$$

$$s_t \geq y_t - y_{t-1} \quad t \in 2,...,N_t \tag{S5}$$

$$s_t \geq y_t - y_{N_t} \quad t = 1 \tag{S6}$$

Equation S1 relates the natural gas requirement to the NGCC power production. Coefficients c_1^{PP} and c_2^{PP} are determined via linear regression to the Aspen Plus model. y_t is a binary variable denoting if the power plant is on ($y_t = 1$) or off ($y_t = 0$). In equation S2, a minimum stable loading operation with respect to the maximum capacity is enforced. Equation S3 ensures that no power is produced by the NGCC plant when it is off. Equation S4 relates the total flue gas flow rate to the natural gas flowrate, with $c^{NG,PP}$ determined from the Aspen Plus model. Equations S5 and S6 track start-up operation with a binary s_t that equals 1 when the power plant switches from off to on between successive time points. Equations S5 and S6 determine the binary variable s_t which tracks periods of start up of the NGCC plant and is used to calculate operational expenditures due to start-up. Here, Equation S6 defines the constraint for the first period by looking back at the state of the power plant at the last operational time step (N_t) of the year.

S1.2 Solid streams

The following set of equations describe the mole balance on streams consisting only of solid components. Impurities that that may be part of the feed limestone such as other metal oxides are assumed to be negligible.

$$j_s = \{CaO, CaCO_3\} \tag{S7}$$
$$i_s = \{1,2,3,4,5,6\} \tag{S8}$$
$$F_{i_s,t}^{tot,s} = \sum_{j \in j_s} F_{i,j_s,t}^{s} \quad t \in \{1,...,N_t\} \tag{S9}$$
$$F_{2,j_s,t}^{s} = F_{1,j_s,t}^{s} + F_{6,j_s,t}^{s} \quad t \in \{1,...,N_t\} \tag{S10}$$
$$F_{3,j_s,t}^{s} = F_{4,j_s,t}^{s} + F_{5,j_s,t}^{s} \quad t \in \{1,...,N_t\}, \tag{S11}$$

Where stream 1 is the feed $CaCO_3$, stream 2 is the calciner inlet, stream 3 is the calciner outlet, stream 4 is the CaO stream sent to DAC, stream 5 is the CaO sent to the carbonator, and stream 6 is the carbonator solids outlet recycled to the calciner. The splitter after the calciner is modelled as

$$F_{5,j_s,t}^{s} = \gamma_t F_{3,j_s,t}^{s} \quad \gamma \in [0,1], \quad t \in \{1,...,N_t\} \tag{S12}$$

where γ is the fraction of solids sent to the carbonator (the remainder 1-γ is sent to the DAC unit). This introduces two bilinear terms to the optimization. While the addition of generalized reduction constraints can lead to a tighter relaxation of the non-convex formulation[4] (in this case, adding the redundant constraint $F_{4,j_s,t}^{s} = (1-\gamma_t)F_{3,j_s,t}^{s}$), it was found that the performance of the optimization algorithm is worsened significantly when adding such constraints. This is in agreement with the recent work of Karia et al.[5] who found that appending structurally redundant quadratic constraints worsened solver performance of mixed-integer quadratically-constrained programs for a variety of global solvers.

The following equations are used to model the reactions in the solid phase ($CaCO_3$ <-> CaO + CO_2) in the calciner and carbonator:

$$F_{3,CaCO_3,t}^{s} = F_{2,CaCO_3,t}^{s} - \zeta_t^{calc} \quad t \in \{1,...,N_t\} \tag{S13}$$
$$F_{3,CaO,t}^{s} = F_{2,CaO,t}^{s} + \zeta_t^{calc} \quad t \in \{1,...,N_t\} \tag{S14}$$
$$F_{6,CaCO_3,t}^{s} = F_{5,CaCO_3,t}^{s} + \zeta_t^{carb} \quad t \in \{1,...,N_t\} \tag{S15}$$
$$F_{6,CaO,t}^{s} = F_{5,CaO,t}^{s} - \zeta_t^{carb} \quad t \in \{1,...,N_t\}, \tag{S16}$$

Where ζ_t^{calc} and ζ_t^{carb} are the extent of reaction in the calciner and the carbonator respectively. These are written in terms of the reactant conversions,

$$\zeta_t^{calc} = X^{calc} F_{2,CaCO_3,t}^{s} \quad t \in \{1,...,N_t\} \tag{S17}$$
$$\zeta_t^{carb} = \bar{X}_t^{carb} F_{5,CaO,t}^{s} \quad t \in \{1,...,N_t\} \tag{S18}$$

We assume complete conversion in the calciner ($X^{calc} = 1$). This removes a bilinear term in equation S12 since $F_{5,CaCO_3,t}^{s} = \gamma_t F_{3,CaCO_3,t}^{s}$ becomes redundant when $F_{3,CaCO_3,t}^{s} = 0$. The average conversion in the carbonator is given by

$$\bar{X}_t^{carb}(1 - f_m\gamma_t) = (1-\gamma_t)f_m(1-f_w) + f_w(1-f_m\gamma_t) \quad t \in \{1,...,N_t\} \tag{S19}$$

Where f_m and f_w are parameters determined from experimental data[1]. The derivation of this equation is described in detail in section S4.

S1.3 Gas/Liquid streams

The gas streams before the membrane unit and their components are modeled as

$$i_{gl} = \{7,8,9,10,11,12,13,14,15,16\} \tag{S20}$$
$$j_{gl} = \{CO_2, N_2, H_2O, O_2, CH_4\} \tag{S21}$$
$$F_{i_{gl},t}^{tot,gl} = \sum_{j \in j_{gl}} F_{i,j,t}^{gl} \quad t \in \{1,...,N_t\} \tag{S22}$$

$$z^{gl}_{i_{gl},j_{gl},t} = \frac{F^{gl}_{i_{gl},j_{gl},t}}{F^{tot,gl}_{i_{gl},t}} \quad t \in \{1,...,N_t\} \tag{S23}$$

(S24)

where we have assumed that the CO_2, N_2, H_2O, O_2 and CH_4 are the only major components. A splitter is modeled to determine how much flue gas to send to the calciner or carbonator. Since the flue gas composition does not change, it can be modelled using a single bilinear term

$$F^{gl}_{7,j,t} = F^{gl}_{8,j,t} + F^{gl}_{9,j,t} \quad j \in \quad j_{gl} \quad t \in \{1,...,N_t\} \tag{S25}$$

$$F^{gl}_{9,CO2,t} = \phi_t F^{gl}_{7,CO2,t} \quad \phi \in [0,1] \quad t \in \{1,...,N_t\} \tag{S26}$$

$$F^{gl}_{j,O_2,t} = z^{gl}_{j,O_2} F^{tot,gl}_{j,t} \quad j \in \{8,9\} \quad t \in \{1,...,N_t\} \tag{S27}$$

$$F^{gl}_{j,H2O,t} = z^{gl}_{j,H_2O} F^{tot,gl}_{j,t} \quad j \in \{8,9\} \quad t \in \{1,...,N_t\} \tag{S28}$$

$$F^{gl}_{j,N2,t} = z^{gl}_{j,N_2} F^{tot,gl}_{j,t}, \quad j \in \{8,9\} \quad t \in \{1,...,N_t\} \tag{S29}$$

where ϕ is the split fraction sent to the carbonator, and z^{gl}_{j,O_2}, z^{gl}_{j,H_2O}, z^{gl}_{j,N_2} are fixed compositions of the NGCC flue gas. The mole balance around the calciner unit is given by

$$\zeta^{comb}_t = F^{gl}_{13,CH_4,t} \quad t \in \{1,...,N_t\} \tag{S30}$$

$$F^{gl}_{14,CH_4,t} = F^{gl}_{13,CH_4,t} - \zeta^{comb}_t \quad t \in \{1,...,N_t\} \tag{S31}$$

$$F^{gl}_{14,O_2,t} = F^{gl}_{8,O_2,t} + F^{gl}_{11,O_2,t} + F^{gl}_{12,O_2,t} - 2\zeta^{comb}_t \quad t \in \{1,...,N_t\} \tag{S32}$$

$$F^{gl}_{14,CO_2,t} = F^{gl}_{8,CO_2,t} + \zeta^{comb}_t + \zeta^{calc}_t \quad t \in \{1,...,N_t\} \tag{S33}$$

$$F^{gl}_{14,H_2O,t} = F^{gl}_{8,H_2O,t} + 2\zeta^{comb}_t \quad t \in \{1,...,N_t\} \tag{S34}$$

$$F^{gl}_{14,N_2,t} = F^{gl}_{8,N_2,t} + F^{gl}_{11,N_2,t} + F^{gl}_{12,N_2,t} \quad t \in \{1,...,N_t\}, \tag{S35}$$

where we have assumed complete combustion of natural gas (i.e., Equation S31 = 0). The oxygen requirement is determined by specifying a fixed amount of excess oxygen:

$$F^{gl}_{8,O_2,t} + F^{gl}_{11,O_2,t} + F^{gl}_{12,O_2,t} = (1 + c^{excess_{O_2}})(2\zeta^{comb}_t) \quad t \in \{1,...,N_t\}. \tag{S36}$$

The mole fraction of oxygen fed to the calciner has an upper bound specified by the rotary kiln vendor to limit the flame temperature, this specification is ensured by adding the inequality

$$\sum_{i \in \{8,11,12,13\}} F^{gl}_{i,O_2,t} \leq z^{max,calciner}_{O_2} \sum_{i \in \{8,11,12,13\}} F^{tot,gl}_{i,t} \quad t \in \{1,...,N_t\}, \tag{S37}$$

where $z^{max,calciner}_{O_2}$ is the upper limit on the O_2 mole fraction. The mass balance around the carbonator is given by the following equations

$$F^{gl}_{10,j,t} = F^{gl}_{9,j,t} \quad j \in O_2, H_2O, CH_4 \quad t \in \{1,...,N_t\} \tag{S38}$$

$$F^{gl}_{10,N_2,t} = F^{gl}_{9,N_2,t} + F^{gl}_{23,N_2,t} \quad t \in \{1,...,N_t\} \tag{S39}$$

$$F^{gl}_{10,CO_2,t} = F^{gl}_{9,CO_2,t} + F^{gl}_{23,CO_2,t} - \zeta^{carb}_t \quad t \in \{1,...,N_t\} \tag{S40}$$

$$F^{gl}_{10,CO_2,t} = (1 - X^{carb,CO_2})(F^{gl}_{9,CO_2,t} + F^{gl}_{23,CO_2,t}) \quad t \in \{1,...,N_t\}, \tag{S41}$$

where X^{carb,CO_2} is the fractional conversion of total CO_2 entering the carbonator. The calciner off gas is quenched before entering the HRSG, then dried

$$F^{gl}_{15,j,t} = F^{gl}_{14,j,t} \quad j \in \{O_2, CH_4, CO_2, N_2\} \quad t \in \{1,...,N_t\} \tag{S42}$$

$$F^{gl}_{15,H_2O,t} = F^{gl}_{14,H_2O,t} + c^{quench} F^{tot,gl}_{14,t} \quad t \in \{1,...,N_t\} \tag{S43}$$

$$F^{gl}_{16,j,t} = F^{gl}_{15,j,t} \quad j \in \{O_2, CH_4, CO_2, N_2\} \quad t \in \{1,...,N_t\} \tag{S44}$$

$$F^{gl}_{16,H_2O,t} = c^{waterremoval} F^{gl}_{15,H_2O,t} \quad t \in \{1,...,N_t\}, \tag{S45}$$

where c^{quench} and $c^{dryer,knockout}$ are linear coefficients determined from sensitivity analyses carried out on the Aspen model. Before the membrane compression stage, CH_4,H_2O and O_2 are reduced to trace amounts. Thus, only the binary mixture of CO_2 and N_2 are considered for streams 17-24.

$$i_b = \{17, 18, 19, 20, 21, 22, 23, 24\} \tag{S46}$$

$$j_b = \{CO_2, N_2\} \tag{S47}$$

$$F^{tot,b}_{i_b,t} = \sum_{j_b} F^b_{i_b,j_b,t} \quad t \in \{1,...,N_t\} \tag{S48}$$

$$F^b_{17,j_b,t} = F^b_{16,j,t} \quad t \in \{1,...,N_t\} \tag{S49}$$

$$z^b_{i_b,j_b,t} = \frac{F^b_{i_b,j_b,t}}{F^{tot,b}_{i_b,t}} \quad t \in \{1,...,N_t\} \tag{S50}$$

The mole balance around the membrane is given by:

$$F^b_{17,j_b,t} = F^b_{18,j_b,t} + F^b_{19,j_b,t} \quad t \in \{1,...,N_t\} \tag{S51}$$

The compositions of the permeate and retentate streams are given by

$$y_{f,CO_2,t} = z^b_{17,CO_2,t} \quad t \in \{1,...,N_t\} \tag{S52}$$

$$\bar{\sigma}_t = \frac{Perm_{CO_2} A}{F^{tot,b}_{17,t}} \quad t \in \{1,...,N_t\} \tag{S53}$$

$$y_{CO_2,p,t} = z^b_{19,CO_2,t} = f(\bar{\sigma}, P_t, y_{f,CO_2}) \quad t \in \{1,...,N_t\} \tag{S54}$$

$$y_{CO_2,r,t} = z^b_{18,CO_2,t} = g(\bar{\sigma}, P_t, y_{f,CO_2,t}) \quad t \in \{1,...,N_t\} \tag{S55}$$

$$F^b_{19,CO_2,t} = y_{CO_2,p,t} F^{tot,b}_{19,t} \quad t \in \{1,...,N_t\} \tag{S56}$$

$$F^b_{18,CO_2,t} = y_{CO_2,r,t} F^{tot,b}_{18,t} \quad t \in \{1,...,N_t\} \tag{S57}$$

Where functions f and g are determined from the surrogate model development procedure described in section S6, and $y_{CO_2,p,t}$, $y_{CO_2,r,t}$ are the CO_2 mole fractions in the permeate and retentate streams respectively . The overall component balance around the CPU unit is given by

$$F^b_{19,j_b,t} = F^b_{20,j_b,t} + F^b_{21,j_b,t} \quad t \in \{1,...,N_t\}. \tag{S58}$$

A design specification on the purity of the exported CO_2 steam is imposed

$$F^b_{21,CO_2,t} = c^{z^{21}_{CO_2}} F^{tot,b}_{21,t} \quad t \in \{1,...,N_t\}, \tag{S59}$$

where $c^{z^{21}_{CO_2}}$ is the the CO_2 purity. The total flow rate of high purity CO_2 sent to sequestration is given by

$$F^{tot,b}_{21,t} = c^b_{19,CO_2} F^b_{19,CO_2,t} + c^{tot,b}_{19,CO_2} F^{tot,b}_{19,t} \quad t \in \{1,...,N_t\}, \tag{S60}$$

where c^b_{19,CO_2} and $c^{tot,b}_{19,CO_2}$ are coefficients determined via linear regression to the output of the Aspen Plus model simulations for a range of permeate flowrate and compositions. Due to imperfect separation of CO_2 in the membrane and CPU units, the retentate and top-product of the CPU distillation column are mixed and portion of these gases are recycled to the carbonator:

$$F^b_{22,j_b,t} = F^b_{18,j_b,t} + F^b_{20,j_b,t} \quad t \in \{1,...,N_t\} \tag{S61}$$

$$F^b_{22,j_b,t} = F^b_{23,j_b,t} + F^b_{24,j_b,t} \quad t \in \{1,...,N_t\} \tag{S62}$$

$$F^b_{23,j_b,t} = \alpha_t F^b_{22,j_b,t} \quad \alpha_t \in [0,1] \quad t \in \{1,...,N_t\}, \tag{S63}$$

where α is the fraction of gases recycled to the carbonator, (the remainder 1-α is vented to the atmosphere).

S1.4 DAC storage

A solids storage device before the DAC unit is modeled in order to reduce the capacity requirement of the DAC system.

$$nCaODAC_t = nCaODAC_{t-1} + F^s_{4,CaO,t} - CaO_{use} \quad t \in \{2,...,N_t\} \tag{S64}$$

$$nCaODAC_{t=1} \leq nCaODAC_{t=N_t} \tag{S65}$$

$$nCaODAC_t = nCaODAC_{t-23} \quad \text{if} \quad t(\quad \text{mod } 24) = 1, \quad t \in \{1,...,N_t\} \tag{S66}$$

Equation S64 models the accumulation of moles in the storage unit. Equation S65 limits the initial storage to be no more than the storage at the last time point. Equation S66 ensures that the amount of CaO in the storage device is the same at the start and end of each 24 hr period.

S1.5 Heat and Work

Excess heat from the carbonator off-gas (stream 10 in Figure 1 of the main text) is used to provide heat to the dryer and HRSG. Note that the heat transfer is not depicted in the figure. Furthermore, the HRSG also has a steam cycle for power generation, as explained in detail by Sheha *et al.* [3]. In this work the HRSG and steam cycle are treated as a single unit and labelled 'HRSG'. The temperature and pressure of the inlet streams to the carbonator do not vary in temperature and pressure, however the compositions change. The outlet temperatures from the HRSG are fixed. We assume that the total enthalpies of each stream can be approximated by the pure component enthalpies (i.e., heat of mixing is neglected). The pure component enthalpies $h_{i,j}$ are taken from Aspen. An energy balance around the carbonator, dryer and HRSG gives:

$$\Delta H_t = \sum_{j\in j_{gl}} h_{9,j}F^{gl}_{9,j,t} + \sum_{j\in j_b} h_{23,j}F^{b}_{23,j,t} \tag{S67}$$

$$+ \sum_{j\in j_s} h_{5,j}F^{b}_{5,j,t} - \sum_{j\in j_s} h_{6,j}F^{b}_{6,j,t} - 3600Q^{carb,loss} \quad t\in\{1,...,N_t\} \tag{S68}$$

Where ΔH_t is enthalpy change between the carbonator off-gases (stream 10 in Figure 1 of the main text) and the vented gas from the HRSG and $h_{i,j}$ is the pure component enthalpy for stream i and component j. The heat requirement for the dryer is determined from the inlet flowrate of water:

$$Q^{dryer}_t = c^{Qdryer}F^{gl}_{16,H_2O,t} \quad t\in\{1,...,N_t\} \tag{S69}$$

The calciner off-gases (stream 14) are quenched to 620 $^\circ$ C (stream 15) before the HRSG and exit the HRSG (stream 16) at 180°C. For a complete description of the various operating conditions and design specifications the reader is referred to the work of Sheha *et al.* [3]. The HRSG power can then be determined by the following equation

$$3600(W^{HRSG}_t + Q^{dryer}_t) = c^{\eta^{HRSG}}((c^{T_{15}} - c^{T_{16}})\bar{C}_p F^{tot,gl}_{15,t} + \Delta H_t) \quad t\in\{1,...,N_t\}, \tag{S70}$$

where $c^{\eta^{HRSG}}$ relates the heat transferred for steam generation and power produced from the HRSG, and is determined from the Aspen simulation. The cooling duty requirement for the power plant and CPU system are given as a function of stream 7 and stream 14 as follows:

$$Cduty^{PP}_t = c^{Cduty,PP}F^{tot,gl}_{7,t} \quad t\in\{1,...,N_t\} \tag{S71}$$

$$Cduty^{Carbon8}_t = c^{Cduty,Carbon8}F^{tot,gl}_{14,t} \quad t\in\{1,...,N_t\} \tag{S72}$$

The following expressions are used to compute the power requirements for the VPSA, CPU and DAC units.

$$W^{VPSA}_t = c^{WVPSA}F^{tot,gl}_{11,t} \quad t\in\{1,...,N_t\} \tag{S73}$$

$$W^{CPU}_t = c^{WCPU}F^{tot,b}_{19,t} \quad t\in\{1,...,N_t\} \tag{S74}$$

$$W^{DAC} = c^{WDAC}CaO_{use} \tag{S75}$$

The compressor before the membrane is modeled in the Aspen model with 8 stages and inter-stage cooling. We approximate the compression work using the equation for isothermal compression of an ideal gas, and scale the equation to match the compression work given by the Aspen simulation.

$$W^{Compressor}_t = c^{comp}Rc^{T_{16}}\log(P_t/c^{P_0})/3600 \quad t\in\{1,...,N_t\} \tag{S76}$$

A linear regression is performed to approximate $\ln P_t$, with coefficients shown in Table S2.

$$\ln P_t = c^{lnP}_1 P_t + c^{lnP}_2 \quad t\in\{1,...,N_t\} \tag{S77}$$

To determine a relationship between the calciner solids inputs, fuel and oxygen requirements, a correlation was developed, determined by conducting sensitivity analyses on the Aspen model. Since all relevant streams are at a fixed temperature, the following linear correlation approximates the energy balance around the calciner

$$c^{tot,gl}_{11}F^{tot,gl}_{11,t} + c^{tot,gl}_{8}F^{tot,gl}_{8,t} + c^{tot,gl}_{12}F^{tot,gl}_{12,t} \tag{S78}$$

$$= c^{s}_{1}F^{tot,s}_{1,t} + c^{s}_{6,CaCO_3}F^{s}_{6,CaCO3,t} + c^{s}_{6,CaO}F^{s}_{6,CaO,t} \quad t\in\{1,...,N_t\}. \tag{S79}$$

S1.6 Variable bounds

Variables are bounded according to their context, e.g., flow rates are defined as positive reals and split fractions are constrained between 0 and 1. In Table S3 we show the additional variable bounds that are added to ensure that the optimization problem is bounded and that practical solutions are obtained. Other variables are bounded implicitly from the process constraints.

S1.7 Feed compositions

As evidenced from the Aspen model of the NGCC plant[3], the composition of the flue gas (stream 7) does not change significantly with loading within the range of stable operation. The compositions of the other inlet streams are also invariant with time (streams 1,11,12 and 13). The inlet compositions are therefore fixed as parameters in the model, and are detailed in table S2.

Table S3 Variable bounds used in the optimization model.

Variable	Definition	Units	Lower Bound	Upper bound
W_t^{PP}	Net power output from NGCC	GWh	0	$W^{PP,CAP}$
$y_{CO_2,p}$	CO_2 mole fraction in membrane permeate	-	0.55	0.9
$y_{CO_2,r}$	CO_2 mole fraction in membrane retentate	-	0	0.25
$y_{CO_2,f}$	CO_2 mole fraction in membrane feed	-	0.3	0.55
$\bar{\sigma}$	Dimensionless membrane area divided by feed pressure	-	15	50
$flowRatio_u$	Ratio of capacity flow to that of the base case[3]	-	0	5
P_t	Membrane feed and retentate pressure	bar	3	10
$F_{2,t}^{tot,s}$	Total solids to calciner	MMol/hr	0	17

Table S4 Parameters used in the CAPEX calculation. Cost Coeff (c_u) refers to the cost of unit u with base flow bf_u. base Case Flow (bcf_u) is the flowrate provided in the paper of Sheha *et al.*[3]. Cost exponent (e_u) is the exponent used in cost estimation function (Equation S93).

Unit (u)	**Cost Coeff (c_u) ($M)**	**base Flow (bf_u)**	**base Case Flow (bcf_u)**	**cost exponent (e_u)**
Calciner	29.4	0.398 Mmol/hr	17.061 Mmol/hr	0.8
Carbonator	21.6	0.862 Mmol/hr	13.62 Mmol/hr	0.8
DAC	131.9	3.4 Mmol/hr	3.42 Mmol/hr	1
HRSG, turbines+generators	73.2	0.263 GW	0.138 GW	0.8
HRSG, ductwork+stack	105.1	0.110 GW	0.109 GW	0.9
Membrane Compressor	167.2	0.087 GW	0.0559 GW	0.75
Limestone Mill	8.08	0.38 Mmol/hr	3.414 Mmol/hr	0.7
Blower	68.7	42.91 Mmol/hr	42.91 Mmol/hr	0.75
CPU	173.1	40.35 Mmol/hr	18 Mmol/hr	0.75
VPSA	345.1	9.43 Mmol/hr	5.918 Mmol/hr	0.75
BOP Cooling Water	36.3	0.397 GW	1.241 GW	0.6
BOP Feed Water	95.0	0.397 GW	0.397 GW	1
Power Plant	567.0	0.74 GW	0.74 GW	1
DAC storage	9.9	13.4 Mmol	13.4 Mmol	0.7
Membrane	150 ($/m^2)[6]	-	-	-

S2 Process Economics

S2.1 CAPEX

Capacity variables $capFlow_u$ represent the maximum flow associated with each process unit, and are used to approximate the cost. The calciner, carbonator, limestone mill, blower and VPSA are scaled according to the total inlet molar flowrate. The maximum flow over time for is modeled by introducing inequality constraints

$$capFlow_{calciner} \geq F_{2,t}^{tot,s} \quad t \in \{1,..,N_t\} \tag{S80}$$

$$capFlow_{carbonator} \geq F_{5,t}^{tot,s} \quad t \in \{1,..,N_t\} \tag{S81}$$

$$capFlow_{LimestoneMill} \geq F_{1,t}^{tot,s} \quad t \in \{1,..,N_t\} \tag{S82}$$

$$capFlow_{Blower} \geq F_{16,t}^{tot,gl} \quad t \in \{1,..,N_t\} \tag{S83}$$

$$capFlow_{VPSA} \geq F_{11,t}^{tot,gl} \quad t \in \{1,..,N_t\} \tag{S84}$$

It is assumed that the cost of the cryogenic processing unit may be determined only as a function of the total flowrate of the permeate stream exiting the membrane.

$$capFlow_{CPU} \geq F_{19,t}^{tot,b} \quad t \in \{1,..,N_t\} \tag{S85}$$

The costs of the HRSG, membrane compressor and balance of power (BOP) scale with respect to the power and cooling duty. Note that the HRSG and steam cycle for power generation are treated as a single unit and labelled 'HRSG', since the cost of the steam cycle and HRSG both scale with the power output from the aggregated unit. Their capacity variables are defined using

$$capFlow_{HRSG,turbines+generators} \geq W_t^{HRSG} \quad t \in \{1,..,N_t\} \tag{S86}$$

$$capFlow_{HRSG,ductwork+stack} \geq W_t^{HRSG} \quad t \in \{1,..,N_t\} \tag{S87}$$

$$capFlow_{MembraneCompressor} \geq W_t^{Compressor} \quad t \in \{1,..,N_t\} \tag{S88}$$

$$capFlow_{BOPCoolingWater} \geq Cduty_t^{PP} + Cduty_t^{Carbon8} \quad t \in \{1,..,N_t\}. \tag{S89}$$

The cost of CaO storage before the DAC unit is determined from the maximum inventory level ($cap_{DACstorage}$)

$$cap_{DACstorage} \geq nCaODAC_t \quad t \in \{1,..,N_t\} \tag{S90}$$

The calciner capacity is given a suitable upper bound to limit the size of the overall system.

$$capFlow_{calciner} \leq capFlow^{max,calciner} \tag{S91}$$

The following equations are then used to determine the cost of each unit $u \in$ { Calciner, Carbonator, DAC, HRSG turbines+generators, HRSG ductwork + stack, Membrane Compressor, Limestone Mill, Blower, CPU, VPSA, BOP Cooling Water, BOP Feed Water, Power Plant, DAC storage }.

$$flowRatio_u bcf_u = capFlow_u \tag{S92}$$

$$unitCost_u \geq c_u (flowRatio_u \frac{bcf_u}{bf_u})^{e_u} \tag{S93}$$

where bcf_u is the flowrate used in the work of Sheha et al[3], bf_u and c_u are the flow rate cost of a base unit for which the price is known to a good approximation. The cost (c_u) of standard units are determined using Aspen Process Economic Analyzer, and the cost of the calciner, carbonator, and DAC units are determined from specific vendor quotes. Values of c_u are shown in Table S4. Note that these costs include not only the base cost for the equipment, but also direct labor, bare erect cost, Engineering, Construction Management, Home Office & Fees (Eng'g CM, H.O. & Fees) and project contingencies. The flow ratio with respect to the capacity flows in the work of[3] is used instead of the capacity flows for which we have the base cost since we do not expect the size of the units to vary significantly from this design and hence smaller bounds on $flowRatio_u$ may be used. We approximate the right hand side of equation S93 with a piecewise linear correlation with domain breakpoints $\{0, 0.1, 0.3, 0.5, 0.7, 1, 2, 3, 4, 5\}$, i.e., the maximum flowrate may vary between 0 and 5 times the flow used in the base case model. The incremental method ('INC' formulation provided by Pyomo[7,8]) is used to formulate a piecewize linear approximation of the nonlinear function. For the membrane unit, the cost is assumed to scale linearly with the membrane area,

$$unitCost_{membrane} \geq c_{membrane} A, \tag{S94}$$

The cost of the NGCC plant is fixed to that of a 740 MW power plant:

$$unitCost_{PowerPlant} = c_{PowerPlant}. \tag{S95}$$

Finally, the CAPEX is given by

$$CAPEX_{annualized} = CRF \sum_u unitCost_u \tag{S96}$$

where CRF corresponds to the capital recovery factor, that annualizes the capital cost based on the discount rate and lifetime reported in Table S2.

S2.2 Operating cost (OPEX)

In this section we describe the equations used to calculate the fixed and variable OPEX of the process, with parameters shown in Table S1.

The variable OPEX expenditures are given by

$$opex_t^{CPU} = w_t EP_t W_t^{CPU} \tag{S97}$$

$$opex_t^{DAC} = w_t EP_t W^{DAC} \tag{S98}$$

$$opex_t^{Membrane} = w_t EP_t W_t^{Compressor} \tag{S99}$$

$$opex_t^{PowerPlantNG} = w_t fuelPriceF_t^{NG,PP} \tag{S100}$$

$$opex_t^{CalcinerNG} = w_t fuelPriceF_{13,t}^{tot,gl} \tag{S101}$$

$$opex_t^{VPSA} = w_t EP_t W_t^{VPSA} \tag{S102}$$

$$opex_t^{LimestonePurchase} = w_t c^{LimestonePurchase} F_{1,t}^{tot,s} \tag{S103}$$

$$opex_t^{LimestoneDisposal} = w_t c^{LimestoneDisposal} CaO_{use} \tag{S104}$$

$$opex_t^{VentedGasRecycle} = w_t CarbonPriceF_{24,CO_2,t}^{b} \tag{S105}$$

$$opex_t^{VentedGasCarbonator} = w_t CarbonPriceF_{10,CO_2,t}^{b} \tag{S106}$$

$$opex_t^{CO_2Sequestration} = c^{Sequestration} w_t F_{21,CO_2,t}^{b} \tag{S107}$$

$$opex_t^{Startup} = c^{StartUp} w_t s_t W^{PP,CAP} \tag{S108}$$

where w_t are the weights for each representative time step modeled (see section S5) and are scaled such that $\sum_t w_t = 8760$ for annual operation. Summing each term over t gives the annualized OPEX.

$$OPEX_{var,annual} = \sum_u \sum_t opex_t^u \tag{S109}$$

The fixed OPEX is approximated as a linear function of the total CAPEX at the aggregate level

$$OPEX_{fixed,annual} = c_1^{FixedOPEX} + c_2^{FixedOPEX} CAPEX \tag{S110}$$

The annual opex is given by

$$OPEX_{annual} = OPEX_{var,annual} + OPEX_{fixed,annual} \tag{S111}$$

The three revenue streams are from the power generation and CO_2 sequestration

$$revenue_t^{PowerPlant} \leq w_t EP_t W_t^{PP} \tag{S112}$$

$$revenue_t^{HRSG} \leq w_t EP_t W_t^{HRSG} \tag{S113}$$

$$revenue_t^{DAC} \leq X^{CaO,DAC} w_t CarbonPriceCaO_{use} \tag{S114}$$

$$REVENUE_{annual} = \sum_u \sum_t revenue_t^u \tag{S115}$$

S2.3 Objective Function

S2.3.1

The objective function is to maximize the net present value (NPV), which is given by

$$NPV(\$M) = \frac{-CAPEX_{annualized} + (REVENUE_{annual} - OPEX_{annual})}{CRF}. \tag{S116}$$

S3 Demand-based optimization model

In this section, we introduce the optimization problem formulated to analyze the demand-based optimization scenario, different from the approach that directly uses the electricity price profile as discussed in section S2. Here, we consider the following technologies:

- NGCC: standalone NGCC system, described by equations S1-S6 with the same CAPEX parameters and operational costs associated with natural gas price and carbon emissions.
- Solar: solar electricity generation facility with CAPEX parameters described in table S4, with availability factors $\rho_{solar,t}$ forecast for the PJM West region.
- Wind: wind electricity generation facility with CAPEX parameters described in table S4, with availability factors $\rho_{wind,t}$ forecast for the PJM West region.
- Battery: battery storage facility with CAPEX parameters described in table S4, with availability factors $\rho_{solar,t}$ forecast for the PJM West region.
- NGCC + Carbon8 + DAC: coupled system for the technology described in this work, as described by equations S1 - S115.

S3.1 K-means clustering

Similar to the K-means clustering on the electricity profiles as described in section S5, which utilizes k-means clustering exclusively on electricity price profiles, the methodology used in the demand-based optimization integrates a dataset encompassing demand, solar availability ($\rho_{solar,t}$), and wind availability ($\rho_{wind,t}$). This approach involves normalizing these three features, representing each day as a single data point in a higher dimensional space. The k-means algorithm is then applied to this dataset to identify distinct clusters. Each cluster represents a typical pattern across the three dimensions. This method not only accounts for the variability in demand but also incorporates the fluctuating nature of renewable energy sources, thus enabling a more accurate representation of the energy system dynamics.

S3.2 Optimization problem

The optimization problem is written as a cost minimization as follows.

$$\begin{aligned}
\min \quad & (CAPEX_{annualized} + OPEX_{annual} - REVENUE_{annual}) + && \text{(S117)}\\
& CAPEX_{annualized,NGCC} - OPEX_{annual,NGCC} && \text{(S118)}\\
& + (\sum_{g\in G} c_g^{inv}\Theta_g + \sum_{s\in S} a_s^{inv,e}\Phi_s^e + \sum_{s\in S} a_s^{inv,p}\Phi_s^p \\
& + \sum_{t\in T}\sum_{g\in G} c_g^{op}\theta_{g,t}w_t + \sum_{t\in T}\sum_{s\in S} a_s^{op}\phi_{s,t}^d w_t \\
& + \sum_{g\in G} fOPEX_g\Theta_g + \sum_{s\in S} fOPEX_s(\Phi_s^e + \Phi_s^p)) && \text{(S119)}
\end{aligned}$$

Subject to:

$$\sum_{g\in G}\theta_{g,t} + \sum_{s\in S}\phi_{s,t}^d - \sum_{s\in S}\phi_{s,t}^c + netPower_{FLECCS,t} = D_t \quad \forall t \in T \tag{S120}$$

$$\theta_{g,t} \leq \rho_{g,t}\Theta_g \quad \forall g \in G, t \in T \tag{S121}$$

$$\phi^e_{s,t} = \phi^e_{s,t-1} + \eta^c_s \phi^c_{s,t} - \frac{1}{\eta^d_s}\phi^d_{s,t} \quad \forall s \in S, t \in T | t \neq 1 \tag{S122}$$

$$\phi^e_{s,t} = \phi^e_{s,\bar{T}} + \eta^c_s \phi^c_{s,t} - \frac{1}{\eta^d_s}\phi^d_{s,t} \quad \forall s \in S, t = 1 \tag{S123}$$

$$\phi^c_{s,t} \leq \Phi^p_s \quad \forall s \in S, t \in T \tag{S124}$$

$$\phi^d_{s,t} \leq \Phi^p_s \quad \forall s \in S, t \in T \tag{S125}$$

$$\phi^e_{s,t} \leq \Phi^e_s \quad \forall s \in S, t \in T \tag{S126}$$

The CAPEX ($CAPEX_{annualized,NGCC}$) and OPEX ($OPEX_{annual,NGCC}$) for the standalone NGCC system are computed from the same process model for the NGCC plant, as described in section S1.1, and the same CAPEX parameters as described in section S2.1. The first three bracketed terms in the objective function are used to compute the annualized cost of the NGCC + Carbon8 + DAC system, as described in sections S1 and S2. The last bracketed terms in the objective function are used to compute the annualized cost of the other competing generation and storage technologies, with parameters and variables described in tables S2 and S1 respectively. For this case study, we choose $g \in \{wind, solar\}$ and only battery storage ($s \in \{battery\}$). Standalone NGCC is treated separately to account for varying heat rates at part loading, as captured by the equations in section S1.1.

Model Variables

Table S5 List of variables used within the optimization model.

Variable	Description	Units
Θ_g	Installed capacity of power generator g	MW
Φ^e_s	Installed energy capacity of energy storage resource s	MWh
Φ^p_s	Installed charge/discharge power capacity of energy storage resource s	MW
$\phi^d_{s,t}$	Discharging power injected by storage resource s in time step t	MW
$\phi^c_{s,t}$	Charging power consumed by storage resource s in time step t	MW
$\phi^e_{s,t}$	Energy storage level in storage resource s in time step t	MWh
$\theta_{g,t}$	Power output by generator g in time period t	MW
$netPower_{FLECCS,t}$	Net power of the FLECCS system in time period t	MW

Model Parameters

Table S6 List of Parameters used within the optimization model.

Parameter	Description	Value	Units
c^{inv}_{NGCC}	Investment cost for standalone NGCC	116698	\$ / (MW.yr)
c^{inv}_{solar}	Investment cost for solar	79028	\$ / (MW.yr)
c^{inv}_{wind}	Investment cost for wind	96759	\$ / (MW.yr)
c^{op}_{wind}	Operating cost for wind resource	0	\$ / MWh
c^{op}_{solar}	Operating cost for solar resource	0	\$ / MWh
$a^{inv,e}_{battery}$	Energy investment cost for battery storage	18642	\$ / MWh
$a^{inv,p}_{battery}$	Power investment cost for battery storage	16063	\$ / MW
$a^{op}_{battery}$	Operating cost of battery storage during discharging	0.1	\$ / MWh
$fOPEX_{NGCC}$	Fixed operating expenditure for generator g	27300	\$ / MW-year
$fOPEX_{Wind}$	Fixed operating expenditure for generator g	38950	\$ / MW-year
$fOPEX_{Solar}$	Fixed operating expenditure for generator g	16640	\$ / MW-year
$fOPEX_{Battery}$	Fixed operating expenditure for generator g	4923	\$ / MW-year
$\rho_{g,t}$	Availability factor for generator g in time step t	Determined via k-means clustering	Unitless
$\eta^c_{battery}$	Charging efficiency of battery storage	0.95	Unitless
$\eta^d_{battery}$	Discharging efficiency of battery storage s	0.95	Unitless
D_t	Power demand in each time step t		MW

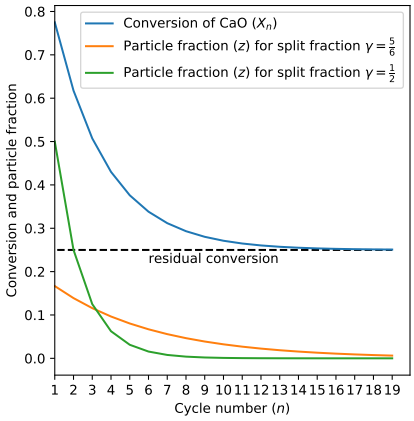

Figure S1 Figure to show the terms in equation S128 for various values of n with $f_m = 0.7$ and $f_w = 0.25$[1].

Table S6 – continued from previous page

Parameter	Description		Units
w_t	Weight of each time step t	Computed from k-means clustering	Unitless

S4 Carbonator Conversion

Here we derive a relationship between the amount of CaO recycled in the calcium looping process and the CaO conversion in the carbonator. This is motivated by the fact that the sorbent capacity of a CaO particle decreases with an increasing number of calcination and carbonation cycles. A critical assumption used in the model is that all CaO particles reach their maximum conversion in the carbonator. This provides an optimistic approximation of the conversion, but avoids needing a detailed model of the reactor. The maximum conversion of CaO for the n^{th} (calcination and carbonation) cycle is given by[1]

$$X_n = f_m^n(1-f_w) + f_w, \tag{S127}$$

with constants determined by curve fitting to experimental data. X_n is the CaO conversion of the n^{th} carbonation. The deactivation constant f_m characterizes the decrease in reaction surface every cycle. The residual conversion, f_w, is the limiting conversion after a large number of cycles (e.g., 30). Summing equation S127 over n and applying the appropriate weights $z(n,\gamma_t)$ (fractions of particles undergoing carbonation at cycle number n) we obtain the average conversion as a function of the split fraction γ:

$$\begin{aligned}\bar{X}(\gamma_t) &= \lim_{N\to\infty} \sum_{n=1}^{N} X_n z(n,\gamma_t) \\ &= \lim_{N\to\infty} \frac{1-\gamma_t}{1-\gamma^N} \sum_{n=1}^{N} (f_m^n(1-f_w)+f_w)\gamma_t^{n-1} \\ &= \frac{(1-\gamma_t)f_m(1-f_w)}{1-f_m\gamma_t} + f_w\end{aligned} \tag{S128}$$

Where $z(n,\gamma_t)$ is the fraction of particles undergoing carbonation at cycle number n. By multiplying through by $(1-f_m\gamma_t)$ we obtain a constraint involving only bilinear terms that is used in the optimization model along with equation S18. In Figure S1 we show the conversion per pass ($\bar{X}_n$) and the mole fraction of particles entering each cycle (z). The conversion decreases rapidly at first with increasing cycle number and reaches the residual conversion f_w asymptotically. The smaller the split fraction, the more the particle distribution is shifted to lower cycle numbers. The particle fraction decreases more rapidly with n at lower values of γ. Specific values of f_m and f_w are chosen to match an operating point given by the carbonator vendor (average conversion of 0.65 at a split fraction $\gamma = 0.5$), and correspond to the correlated data of[1] for Purbeck limestone calcined at 1023 K and particle size between 850 and 1000 μm.

In Figure S2 we show the average conversion for various values of the split fraction. As the split fraction approaches 1, all particles are recycled infinitely and the average conversion approaches f_w, implying that it may be possible to operate without any fresh feed at the expense of lower conversion per cycle. There are therefore feasible solutions to the optimization model where the limestone milling and DAC units are not built, but the calcium loop and downstream separations units are built similar to a standard calcium-looping carbon capture process without DAC, with full recycle of the calcined solids to the carbonator.

S5 Reducing the number of discrete time points

The k-means clustering algorithm used to determine representative days and their corresponding weights is described in in Algorithm 7.

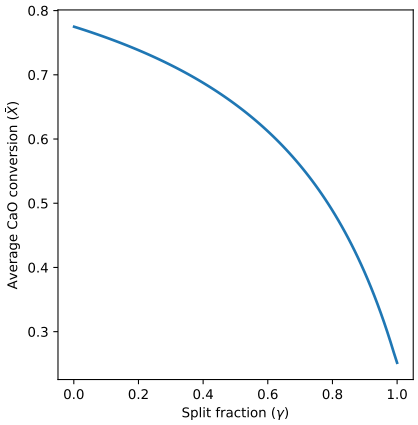

Figure S2 Modeled average CaO conversion as a function of solids split fraction γ, for Purbeck limestone with diameter 850-1000 micrometers[1].

Algorithm 1 Algorithm used to reduce the number of discrete time points

input:
- Electricity price profile EP_t^*, $t \in [1,...,N_t]$, (N_t default 8760)
- Number of hours in a representative period, N_p (default 24)
- Number of clusters, N_c (default 30)
- Number of centroid seeds N_s (default 1000)

output:
- New electricity price profile EP_t.
- Vector of corresponding weights w_t

begin

1. Split EP_t into consecutive periods of length N_p. If $N_t \mod N_p \neq 0$ then remove the trailing days.

2. Determine N_c centroids and their corresponding weights w_t using k-means clustering (scikitlearn KMeans algorithm) with N_s random seeds.

3. For each centroid returned by the k-means algorithm, determine the period from the original profile that minimizes the L2 norm between that period and the centroid.

4. Scale the weights such that $\sum_t w_t EP_t = \sum_t EP_t^*$, i.e., the approximate profile has the same average price as the true profile.

end

S6 Membrane surrogate model

The process consists of a single-stage membrane that is used to purify the gas stream to a suitable level before the cryogenic processing unit. In previous work[3], a model for the membrane was developed that uses the cross-plug flow assumption and determines the compositions and flowrates of the permeate and retentate as a function of the design and operational degrees of freedom, namely the membrane area, A, the flow rate and composition of the feed to the membrane (stream 17), and the feed pressure (P_t). It is assumed that there is no pressure drop on the retentate side, the process is isothermal, and the pressure of the permeate stream is fixed to 1 bar. Furthermore, since all components other than CO_2 and N_2 are reduced to trace amounts before the membrane module, only the binary mixture of CO_2 and N_2 is considered. The key operational degree of freedom is the feed pressure (P_t), which is allowed to vary with time in response to varying feed conditions. In Figure S6 we show a schematic of the membrane model.

The cross-plug flow model may be written as an ordinary differential equation in terms of dimensionless quantities as follows[9]. Introducing the dimensionless quantities:

$$\pi = \frac{Perm_{CO_2}}{Perm_{N_2}} \tag{S129}$$

$$\kappa = \frac{P_p}{P} \tag{S130}$$

$$\theta = \frac{F_{19}^{tot,b}}{F_{17}^{tot,b}} \tag{S131}$$

$$\omega = \frac{F_{18}^{tot,b}}{F_{17}^{tot,b}} \tag{S132}$$

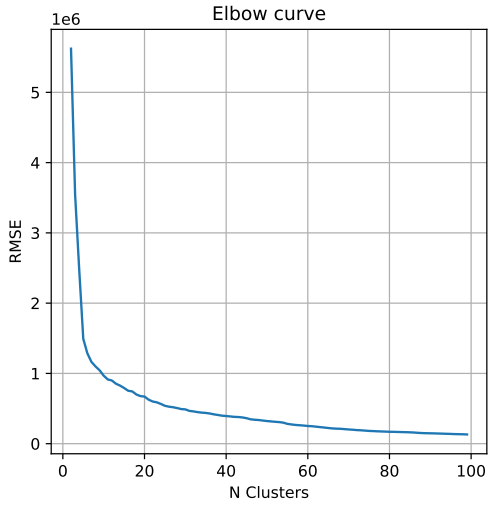

Figure S3 Root mean squared error (RMSE) vs the number of clusters Nc (or representative days) for the MiNg $150 PJM electricity price scenario.

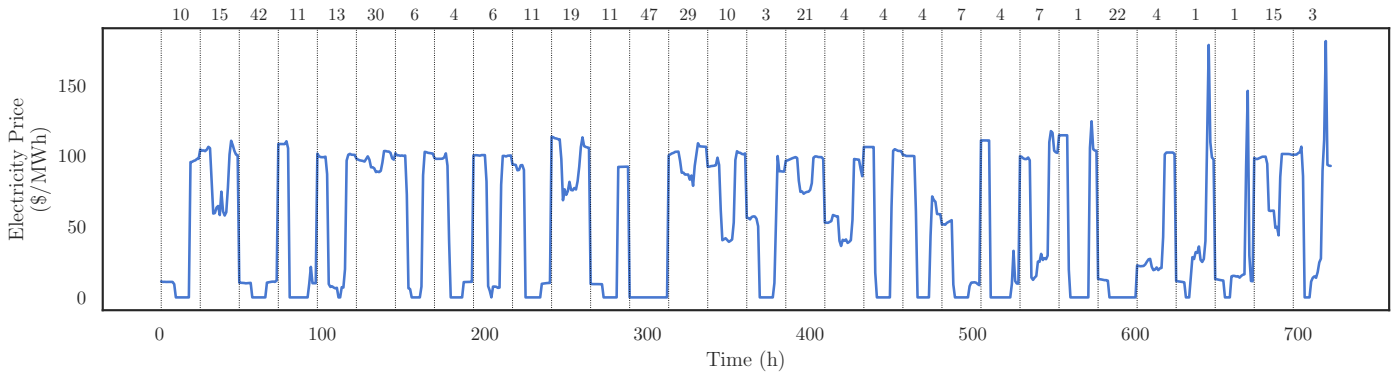

Figure S4 Electricity price profile used to represent the MiNg $150 electricity price scenario. The dotted lines represent the boundary between each characteristic day. The numbers at the top are the corresponding weights w_t that are assigned to each hour in the price profile.

$$\sigma = \frac{Perm_{CO_2} PA}{F_{17}^{tot,b}} \tag{S133}$$

Where π is the ratio of CO_2 permeance to N_2 permeance, θ is the stage cut, $\omega = 1-\theta$, and σ is the dimensionless membrane area. The ODE relating $y_{CO_2,r}$ with σ is given by

$$\frac{dy_{CO_2,r}}{d\sigma} = \frac{(y_{CO_2,r} - y'_{CO_2,p})(y_{CO_2,r} - \kappa y'_{CO_2,p})}{y'_{CO_2,p}\omega}. \tag{S134}$$

$y'_{CO_2,p}$ is the local composition of CO_2 in the permeate stream. The ODE relating ω with σ is given by

$$\frac{d\omega}{d\sigma} = -\frac{y_{CO_2,r} - \kappa y'_{CO_2,p}}{y'_{CO_2,p}}. \tag{S135}$$

$$y'_{CO_2,p} = \frac{1 + (\pi-1)(\kappa + y_{CO_2,r}) - \sqrt{[1+(\pi-1)(\kappa+y_{CO_2,r})]^2 - 4\pi\kappa(\pi-1)y_{CO_2,r}}}{2\beta(\pi-1)} \tag{S136}$$

After integrating equations S134,S135 and S136 the CO_2 purity in the permeate can be expressed as

$$y_{CO_2,p} = \frac{y_{CO_2,f} - \omega(\sigma^{final})y_{CO_2,r}(A)}{1 - \omega(\sigma^{final})}, \tag{S137}$$

Where σ^{final} is the upper limit of integration of the dimensionless membrane area and $\omega(\sigma^{final})$ is the ratio of the retentate flow rate to the feed flow rate evaluated at the final coordinate of integration. The initial conditions are given by

$$y_{CO_2,r}(\sigma = 0) = y_{CO_2,f} \tag{S138}$$

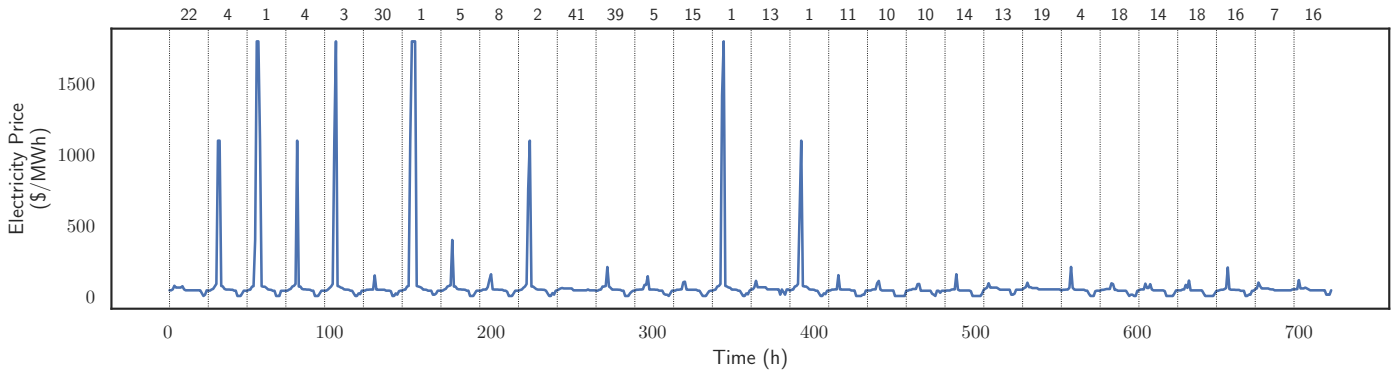

Figure S5 Electricity price profile used to represent the BaseCaseTax electricity price scenario. The dotted lines represent the boundary between each characteristic day. The numbers at the top are the corresponding weights w_t that are assigned to each hour in the price profile.

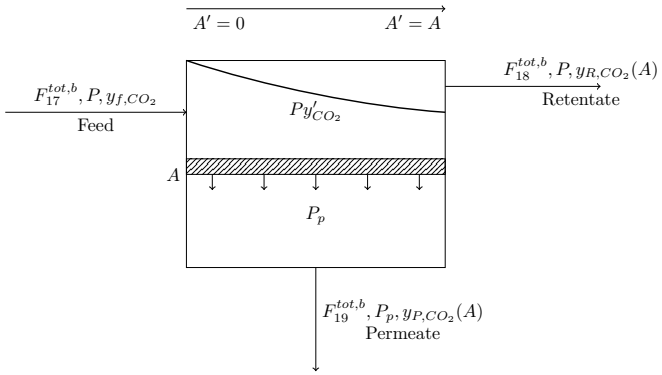

Figure S6 Model schematic for cross- plug flow gas separation membrane based on [9]. Variables with superscript "'" represent local values (which are functions of the area coordinate). $y_{P,CO_2}(A)$ $y_{R,CO_2}(A)$ indicate the mole fractions at the end of the unit (where $A' = A$).

$$\omega(\sigma = 0) = 1 \tag{S139}$$

The permeance values of CO_2 ($Perm_{CO_2}$) and N_2 ($Perm_{N_2}$) are shown in table S1 and reflect the performance of a commercially available membrane [6].

Since representation of the explicit solutions from the ODE in an optimization model is computationally expensive, we developed reduced order functions that approximate the solution to the ODE in the optimization model. In addition to the overall component mass balances (equation S51), two more equations are required to fully specify the membrane unit. We choose to determine functions f and g for the CO_2 mole fractions in the permeate and retentate streams. $\bar{\sigma}$, P and y_{f,CO_2} are chosen as the independent variables, where $\bar{\sigma} = \sigma/P$:

$$y_{CO_2,p} = f(\bar{\sigma}, P, y_{CO_2,f}) \tag{S140}$$

$$y_{CO_2,r} = g(\bar{\sigma}, P, y_{CO_2,f}) \tag{S141}$$

Suitable bounds for the independent variables are chosen as $\bar{\sigma} \in [15,50]$, $P \in [3,10]$, $y_{f,CO_2} \in [0.3,0.55]$. The reduced-order functions are generated using the ALAMO software [10]. The adaptive sampling functionality is employed in order to avoid over-fitting of the model outputs. Bounds on $y_{CO_2,p}$ and $y_{CO_2,r}$ are set to between 0 and 1 to ensure that the resulting model is physical over the domain of input variables. The AICc (corrected Akaike's information criterion) is used as the fitness metric. This rewards goodness of fit and includes a penalty that increases with the number of estimated parameters, resulting in a simpler surrogate model. The following basis functions are specified: monomial power coefficients (-1,0.5,1,2), powers of two terms (1,2), powers of three terms (1), linear functions and a constant. These basis functions are used so that the resultant model does not introduce too many bilinear or quadratic terms when reformulated for the optimization model. The equations that minimize the AICc metric are:

$$y_{CO_2,r} = c_1^{surr}\bar{\sigma} + c_2^{surr}\bar{\sigma}^2 + c_3^{surr} \tag{S142}$$

$$y_{CO_2,p} = c_4^{surr}\bar{\sigma} + c_5^{surr}P + c_6^{surr}y_{f,CO_2} + c_7^{surr}y_{f,CO_2}^2 \tag{S143}$$

The R^2 values for $y_{CO_2,r}$ and $y_{CO_2,p}$ are 0.975 and 0.981 respectively over the 100 sampled points generated during the surrogate model development routine. In Figures S7 and S8 we show the performance of the surrogate model with respect to the ODE model at various feed mole fractions and pressures.

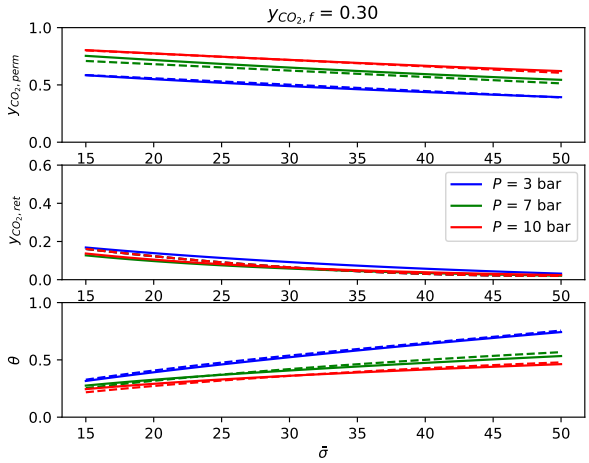

Figure S7 Performance of the membrane surrogate model (dashed lines) with respect to the solution to the ODE model (continuous lines) at feed mole fraction $y_{CO_2,f} = 0.3$

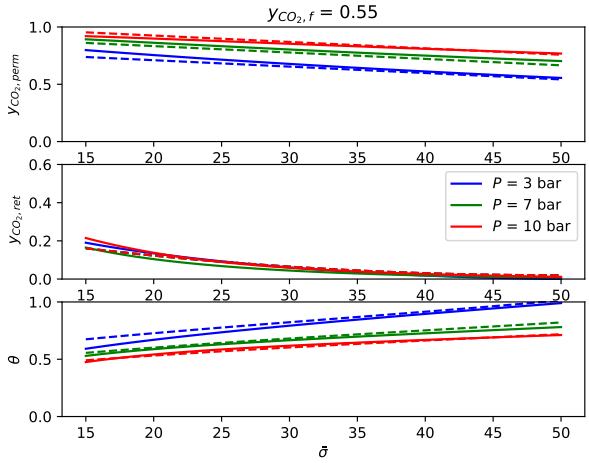

Figure S8 Performance of the membrane surrogate model (dashed lines) with respect to the solution to the ODE model (continuous lines) at feed mole fraction $y_{CO_2,f} = 0.55$

S7 Optimal dispatch of the coupled system at $200/ton carbon price

Figure S9 shows the NPV-optimal dispatch of the coupled system under the MiNg $150 PJM market scenario with carbon price changed to $200/tonne.

S8 Recycling all separation gases to the carbonator

Here we consider the case where we enforce that all off-gases from the membrane (retentate) and CPU (distillation top product) are all recycled back the carbonator for further CO_2 capture, i.e., $\alpha_t = 1$. Operating in such a way may be desirable from an environmental standpoint if net emissions are to be minimized.

In Table S7 we summarize the key metrics for comparison. As expected, the CO_2 capture efficiency is higher in the case where no gases are vented before the carbonator. However, this comes at a cost of $\approx$ $150M in NPV. In Figure S10 we show a comparison of plant operation in the two cases. In the case where all gases are recycled, the solids split fraction γ_t is higher at full loading and the CaO conversion is lower. With a fixed calciner capacity of 17 MMol/hr, the system is able to calcine more feed $CaCO_3$ in the case where we are able to vent some of the recycled gases due to the decreased CaO degradation within the carbonator. Additional benefits of relaxing the constraint on the degree of recycle are that there is less variation in the solids flowrate to the carbonator and there are less periods of part-loading operation of the NGCC plant.

S9 Further information for the MiNg $150 PJM scenario

In this section some further details are provided for the optimal system under the MiNg $150 PJM scenario. The optimal membrane area (A) for this system is 30800 m^2. Tables S8 and S9 show the molar flowrates for each species following the stream numbers in

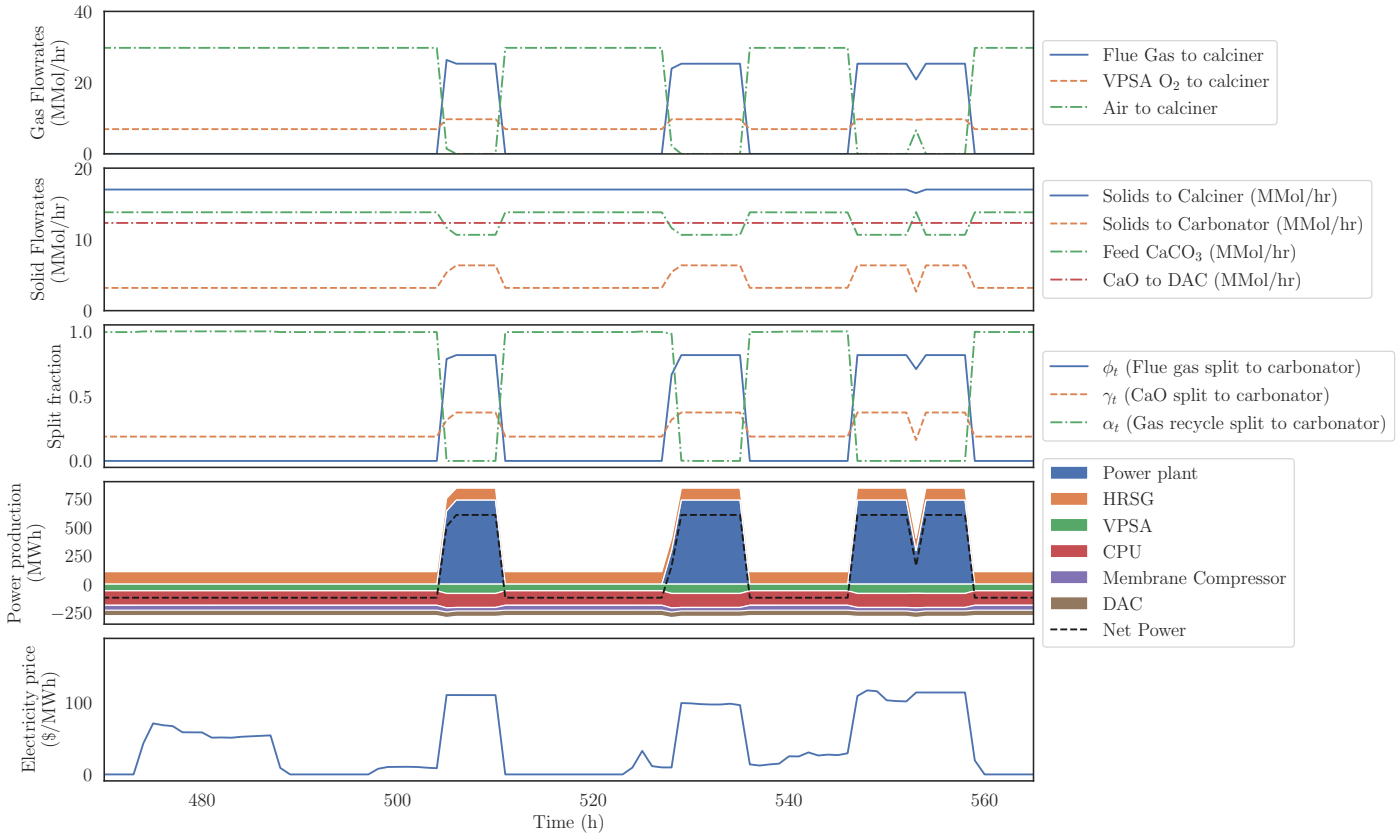

Figure S9 Optimal dispatch of the coupled system under the MiNg $150 PJM market scenario with carbon price changed to $200/tonne.

Fig. 1 of the main text at a particular time when the NGCC is at full ($t = 480$) and part loading ($t = 520$). The breakdown of electricity requirements is shown in table S10. The molar feed flowrates for each major unit operation at maximum capacity are shown in table S11.

Table S7 Comparison of key metrics for optimal MiNg $150 PJM scenario relaxing constraint on recycle. *annual OPEX/ annual net power **annual CO_2 capture rate excluding DAC as a fraction of annual CO_2 input to the system. CO_2 input to the system is defined as the total CO_2 that enters the system, including CO_2 present in calcium carbonate and natural gas.

	Units	Relax Recycle	Fix Recycle
NPV	$bn	1.966	1.817
Upper Bound	$bn	1.970	1.830
Abs. Gap	$bn	0.004	0.013
Rel. Gap (%)	-	0.186	0.710
Fraction of hours NGCC on	-	0.516	0.515
NGCC power	TWh/yr	3.286	3.264
Net power	TWh/yr	2.205	2.303
Cost of power*	$/MW	267	214
CO_2 capture efficiency**	-	0.940	0.987
Net CO_2 emissions	ton/yr	-437	-403

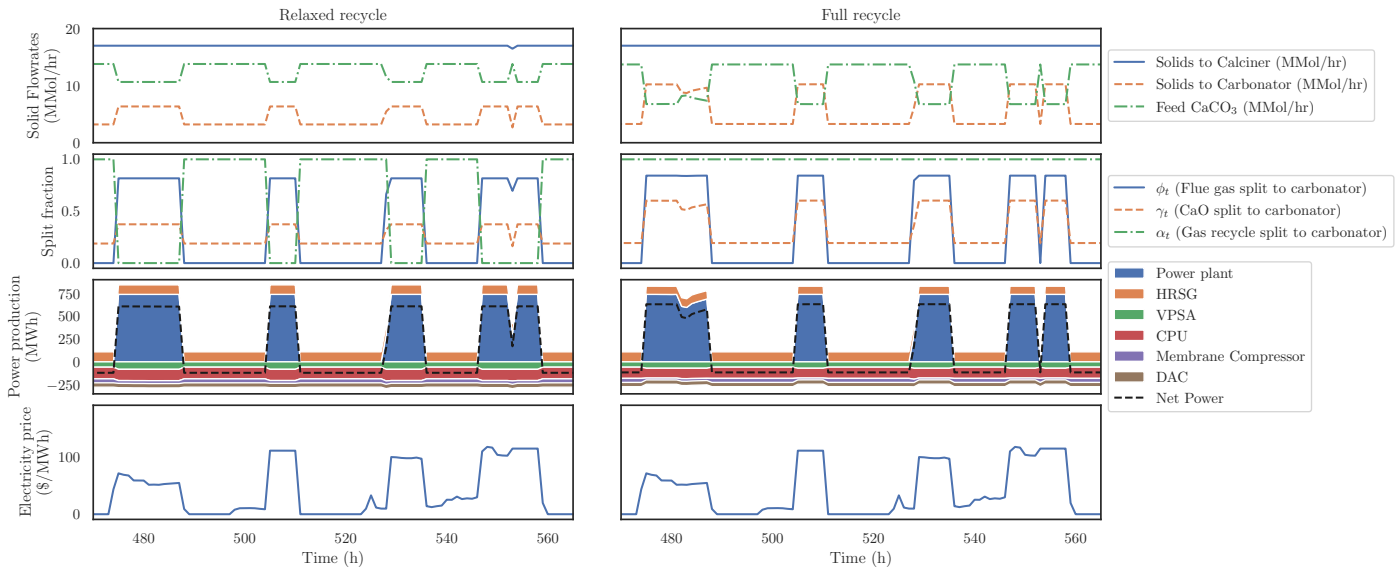

Figure S10 Comparison of optimal dispatch under the MiNg $150 PJM market scenario. Left: the gas recycle split fraction (α_t) is allowed to vary. Right: the gas recycle split fraction (α_t) is fixed to 1 (all gases are recycled).

Table S8 Optimal molar flowrate (Mmol/hr) of each component at Time $t = 480$, corresponding to full NGCC loading. MiNg $150 PJM scenario with the FLECCS system.

Stream	CaO	CaCO3	CO2	O2	H2O	N2	CH4
1	0.0	10.646	-	-	-	-	-
2	1.936	15.064	-	-	-	-	-
3	17.000	0.0	-	-	-	-	-
4	10.646	0.0	-	-	-	-	-
5	6.354	0.0	-	-	-	-	-
6	1.936	4.418	-	-	-	-	-
7	-	-	5.693	16.732	12.206	103.624	0.0
8	-	-	1.043	3.064	2.236	18.979	0.0
9	-	-	4.650	13.667	9.970	84.645	0.0
10	-	-	0.233	13.667	9.970	84.646	0.0
11	-	-	0.0	9.243	0.0	0.486	0.0
12	-	-	0.0	0.000042	0.0	0.000157	0.0
13	-	-	0.0	0.0	0.0	0.0	5.975
14	-	-	22.081	0.358	14.185	19.466	0.0
15	-	-	22.081	0.358	16.748	19.466	0.0
16	-	-	22.081	0.358	0.201	19.466	0.0
17	-	-	22.081	-	-	19.466	-
18	-	-	0.999	-	-	15.618	-
19	-	-	21.082	-	-	3.847	-
20	-	-	1.087	-	-	2.795	-
21	-	-	19.994	-	-	1.052	-
22	-	-	2.087	-	-	18.413	-
23	-	-	0.000107	-	-	0.000942	-
24	-	-	2.087	-	-	18.412	-

Table S9 Optimal molar flowrate (Mmol/hr) of each component at Time $t = 520$, corresponding to zero NGCC loading. MiNg $150 PJM scenario with the FLECCS system.

Stream	CaO	CaCO3	CO2	O2	H2O	N2	CH4
1	0.0	13.795	-	-	-	-	-
2	0.831	16.169	-	-	-	-	-
3	16.999	0.0	-	-	-	-	-
4	13.795	0.0	-	-	-	-	-
5	3.205	0.0	-	-	-	-	-
6	0.831	2.374	-	-	-	-	-
7	-	-	0.0	0.0	0.0	0.0	0.0
8	-	-	0.0	0.0	0.0	0.0	0.0
9	-	-	0.0	0.0	0.0	0.0	0.0
10	-	-	0.125	0.0	0.0	22.775	0.0
11	-	-	0.0	6.605	0.0	0.348	0.0
12	-	-	0.0	6.287	0.0	23.476	0.0
13	-	-	0.0	0.0	0.0	0.0	6.258
14	-	-	22.428	0.376	12.517	23.824	0.0
15	-	-	22.428	0.376	15.220	23.824	0.0
16	-	-	22.428	0.376	0.183	23.824	0.0
17	-	-	22.428	-	-	23.824	-
18	-	-	1.257	-	-	19.307	-
19	-	-	21.171	-	-	4.517	-
20	-	-	1.242	-	-	3.468	-
21	-	-	19.929	-	-	1.049	-
22	-	-	2.499	-	-	22.775	-
23	-	-	2.499	-	-	22.775	-
24	-	-	0.000049	-	-	0.000443	-

Table S10 Electricity Requirements at Times $t = 480$ and $t = 520$, corresponding to full and part loading of the NGCC plant respectively. MiNg $150 PJM scenario with the FLECCS system.

Component	Power (MW) at full NGCC loading	Power (MW) at zero loading
NGCC (WPP)	740.00	0.00
HRSG	104.05	109.72
VPSA	-81.92	-58.54
CPU	-124.05	-127.82
DAC	-47.89	-47.89
Compression	-79.29	-91.40
Total	510.90	-215.93

Table S11 Flowrates to each unit at maximum capacity. MiNg $150 PJM scenario with the FLECCS system.

Unit	Flowrate (Mmol/hr)
Calciner	17.000
Carbonator	6.354
Membrane Compressor	91.401
Limestone Mill	13.795
Membrane Blower	46.810
CPU	25.688
VPSA	9.730
DAC	14.293

Notes and references

[1] P. S. Fennell, R. Pacciani, J. S. Dennis, J. F. Davidson and A. N. Hayhurst, *Energy & Fuels*, 2007, **21**, 2072–2081.

[2] N. Kumar, P. Besuner, S. Lefton, D. Agan and D. Hilleman, *Power plant cycling costs*, National renewable energy lab.(nrel), golden, co (united states) technical report, 2012.

[3] M. Sheha, E. J. Graham, E. Gençer, D. Mallapragada, H. Herzog, P. Cross, J. Custer, A. Goff and I. Cormier, *Computers &; Chemical Engineering*, 2024, **180**, 108472.

[4] J. P. Ruiz and I. E. Grossmann, *Computers & Chemical Engineering*, 2011, **35**, 2729–2740.

[5] T. Karia, C. S. Adjiman and B. Chachuat, *Computers & Chemical Engineering*, 2022, **165**, 107909.

[6] T. Merkel, K. Amo, R. Baker, R. Daniels, B. Friat, Z. He, H. Lin and A. Serbanescu, *Membrane process to sequester CO2 from power plant flue gas*, Membrane technology & research incorporated technical report, 2009.

[7] W. E. Hart, J.-P. Watson and D. L. Woodruff, *Mathematical Programming Computation*, 2011, **3**, 219–260.

[8] M. L. Bynum, G. A. Hackebeil, W. E. Hart, C. D. Laird, B. L. Nicholson, J. D. Siirola, J.-P. Watson and D. L. Woodruff, *Pyomo–optimization modeling in python*, Springer Science & Business Media, 3rd edn., 2021, vol. 67.

[9] M. Gazzani, M. Mazzotti, F. Milella and P. Gabrielli, *ETH Zürich*, 2016.

[10] A. Cozad, N. V. Sahinidis and D. C. Miller, *AIChE Journal*, 2014, **60**, 2211–2227.